

# Wrinkling Phenomena in Neo-Hookean Film/Substrate Bilayers

Yanping Cao

AML,  
Department of Engineering Mechanics,  
Tsinghua University,  
100084, Beijing,  
People's Republic of China

John W. Hutchinson<sup>1</sup>

School of Engineering and Applied Sciences,  
Harvard University,  
Cambridge, MA 02138  
e-mail: hutchinson@husm.harvard.edu

*Wrinkling modes are determined for a two-layer system comprised of a neo-Hookean film bonded to an infinitely deep neo-Hookean substrate with the entire bilayer undergoing compression. The full range of the film/substrate modulus ratio is considered from the limit of a traction-free homogeneous substrate to very stiff films on compliant substrates. The role of substrate prestretch is considered wherein an unstretched film is bonded to a prestretched substrate with wrinkling arising as the stretch in the substrate is relaxed. An exact bifurcation analysis reveals the critical strain in the film at the onset of wrinkling. Numerical simulations carried out within a finite element framework uncover advanced post-bifurcation modes including period-doubling, folding and a newly identified mountain ridge mode. [DOI: 10.1115/1.4005960]*

*Keywords:* wrinkling, neo-Hookean bilayer, bifurcation, period-doubling, folding

## 1 Introduction

A large literature exists reporting short wavelength buckling wrinkles of compressed thin films bonded to thick compliant substrates. Allen's [1] monograph on the mechanics of thin film wrinkling applies to structural systems where the surface film or layer is very stiff compared to the substrate. As applications of soft materials, such as elastomers and gels, grow, there is increasing interest in wrinkling of film/substrate bilayers where both materials are soft and the stiffness ratio of the film to the substrate is not necessarily very large [2]. An important limiting case is surface wrinkling of a compressed homogeneous substrate which Biot [3] analyzed for a neo-Hookean material.

In the first part of this paper, Biot's exact finite strain bifurcation analysis is extended to a bilayer system comprised of a neo-Hookean film bonded to an infinitely deep neo-Hookean substrate. Biot [3] considered several bilayer problems, but not the important case where the film and the substrate are jointly compressed, nor did he consider the role of substrate prestretch. Here, the critical bifurcation strain is obtained for the film/substrate modulus ratio ranging from the limit in which the film and substrate have the same modulus, i.e., a homogeneous substrate, to a very stiff film on a compliant substrate. The role of substrate prestretch is also considered. Substrate prestretching is a technique now widely used by experimentalist to produce compression in the film layer. A thin unstretched film is bonded to a thick prestretched substrate. Then, as the stretch in the substrate is relaxed, the film is compressed and wrinkling occurs. In the second part of the paper, numerical simulations are carried out in plane strain within a finite element framework to uncover advanced post-bifurcation modes including period-doubling, folding and a newly identified mountain ridge mode.

Both materials in the bilayer are incompressible neo-Hookean elastic materials. Quantitative details for other nonlinear elastic material models will differ somewhat from the results present in this paper. Nevertheless, the trends brought out for neo-Hookean materials are expected to have broad applicability. Moreover, when the film is very stiff compared to the substrate, the strain in the film remains small and; thus, it is expected that results in this

range are applicable to any (incompressible) linear elastic film material. The ground state shear modulus of the film is  $\mu_f$  and that of the substrate is  $\mu_s$ . The thickness of the undeformed film is  $h$ ; the substrate is infinitely deep.

Lagrangian coordinates,  $x_i$  ( $i = 1, 3$ ), specifying the locations of material points in the undeformed state of the film are identified in Fig. 1. The coordinate  $x_2$  is perpendicular to the surface of the undeformed bilayer. The surface of the bilayer is traction-free. The stretches in the film and the substrate in the prebifurcation state are uniform and are denoted by  $(\lambda_{1f}, \lambda_{2f}, \lambda_{3f})$  and  $(\lambda_{1s}, \lambda_{2s}, \lambda_{3s})$ , respectively. Prestretches in the substrate, if present, are denoted by  $(\lambda_{1s}^0, \lambda_{2s}^0, \lambda_{3s}^0)$ . Thus, with coordinates  $(\bar{x}_1, \bar{x}_3)$  identifying material points in the interface of the undeformed substrate, the corresponding material points in the interface of the undeformed film to which they are attached are identified by  $x_1 = \lambda_{1s}^0 \bar{x}_1$  and  $x_3 = \lambda_{3s}^0 \bar{x}_3$ . In the uniform prebifurcation state, the stretches in the film and substrate are related to one another by

$$\lambda_{1f} = \lambda_{1s}/\lambda_{1s}^0, \quad \lambda_{2f} = \lambda_{2s}/\lambda_{2s}^0, \quad \lambda_{3f} = \lambda_{3s}/\lambda_{3s}^0 \quad (1)$$

For the combinations of compression and prestretch considered in this paper, the bifurcation mode is an incremental plane strain deformation in the  $(x_1, x_2)$  plane. In all cases, the normal deflection of the surface of the bifurcation mode is proportional to a sinusoidal variation of the form,  $\cos(kx_1) = \cos(2\pi x_1/\ell)$ , where  $\ell = 2\pi/k$  is the wrinkling wavelength referenced to the undeformed film and  $\lambda_{1f}\ell$  is the wavelength in the deformed state.

## 2 Effect of Substrate Prestretch on Wrinkling of Stiff Films on Compliant Substrates

Before considering the neo-Hookean bilayer, a result derived in the Appendix will be presented for wrinkling of a stiff linear elastic film on a compliant neo-Hookean substrate which has undergone a uniform prestretch,  $(\lambda_{1s}^0, \lambda_{2s}^0, \lambda_{3s}^0)$ , prior to attaching the film. The formulas below extend the well known result of Allen [1] by account for the fact that the incremental moduli of the prestretched neo-Hookean substrate change from the ground state and become anisotropic. In the extended result the film is isotropic and linearly elastic with modulus  $E_f$  and Poisson ratio  $\nu_f$ . The formulas apply to arbitrary combinations of substrate prestretch and subsequent film compression under the assumption that the maximum compressive stress in the film is in the

<sup>1</sup>Corresponding author.

Manuscript received August 20, 2011; final manuscript received November 28, 2011; accepted manuscript posted February 13, 2012; published online April 4, 2012. Assoc. Editor: Huajian Gao.

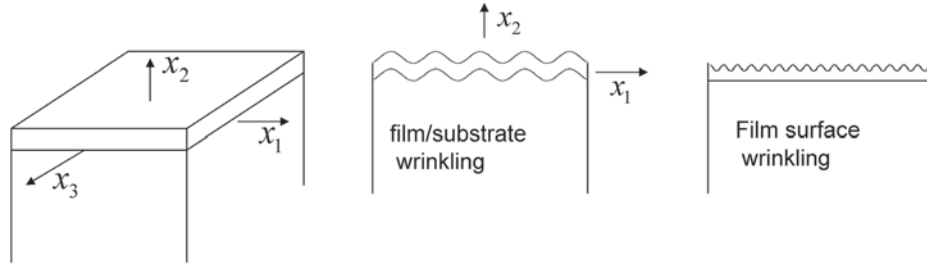


**Fig. 1 Geometry of the film/substrate system and illustrations of wrinkling modes involving interaction between the film and substrate and a shallow surface mode. The cases considered in this paper all correspond to incremental plane strain bifurcations in the  $(x_1, x_2)$  plane.**

1-direction ( $\sigma_{11} = -\sigma$ ). The wrinkling mode is an incremental plane strain mode with normal surface deflection in the form  $u_2 \propto \cos(k_0 x_1)$  with  $x_1$  attached to material points in the undeformed film. The critical stress in the film and the associated wave number are

$$\frac{\sigma}{\bar{E}_f} = \frac{1}{4} \left( \Lambda \frac{3\mu_s}{\bar{\mu}_f} \right)^{2/3}, \quad k_0 h = \left( \Lambda \frac{3\mu_s}{\bar{\mu}_f} \right)^{1/3} \quad \text{with} \quad (2)$$

$$\Lambda = \frac{1}{2\lambda_{3s}^0} (1 + \lambda_{1s}^0)^2 \lambda_{3s}^0$$

Here,  $\bar{E}_f = E_f / (1 - \nu_f^2)$ ,  $\mu_f = E_f / [2(1 + \nu_f)]$  and  $\bar{\mu}_f = \mu_f / [2(1 - \nu_f)]$ . The prestretch factor  $\Lambda$  is unity when there is no prestretch. This result was obtained in Ref. [4] for the special case of plane strain prestretch. This factor is for the neo-Hookean substrate. Nevertheless, the influence of prestretched predicted for this substrate are expected to be illustrative of other elastomeric materials that stiffen when stretched.

### 3 Bifurcation Analysis of Wrinkling of a Bilayer of Neo-Hookean Materials

**3.1 Plane Strain Compression With No Substrate Prestretch.** With no prestretch in the substrate and the bilayer subject to plane strain compression, the prebifurcation stretches satisfy

$$\lambda_{3f} = \lambda_{3s} = 1, \quad \lambda_{1f} = \lambda_{1s} \equiv \lambda_1, \quad \lambda_{2f} = \lambda_{2s} \equiv \lambda_2 = 1/\lambda_1 \quad (3)$$

Compression in the 1-direction is considered with a (nominal) compressive strain defined by

$$\varepsilon = 1 - \lambda_1 \quad (4)$$

By dimensional arguments, the compressive strain at the wrinkling bifurcation,  $\varepsilon_W$ , is only a function of  $\mu_f/\mu_s$ . Details of the bifurcation analysis are given in the Appendix. The film and the substrate are each treated as a continuum with no approximation in the bifurcation analysis. The plot of  $\varepsilon_W$  as a function of  $\mu_f/\mu_s$  is given in Fig. 2. Included in Fig. 2 is the compressive bifurcation strain,  $\varepsilon_0$ , as predicted by Eq. (2) for plane strain:

$$\varepsilon_0 = \frac{1}{4} \left( \Lambda \frac{3\mu_s}{\bar{\mu}_f} \right)^{2/3}, \quad k_0 h = \left( \Lambda \frac{3\mu_s}{\bar{\mu}_f} \right)^{1/3} \quad \text{with} \quad \Lambda = \frac{1}{2} (1 + \lambda_{1s}^0)^2 \quad (5)$$

(with  $\nu_f = 1/2$ ,  $\bar{\mu}_f = \mu_f$  and  $\varepsilon_0 = \sigma/\bar{E}_f$ .) Remarkably, the simple formula, Eq. (5), for  $\varepsilon_0$  with  $\Lambda = 1$ , corresponding to Allen's result for an incompressible film and substrate with no prestretch, retains reasonable accuracy even at modest ratios of the moduli

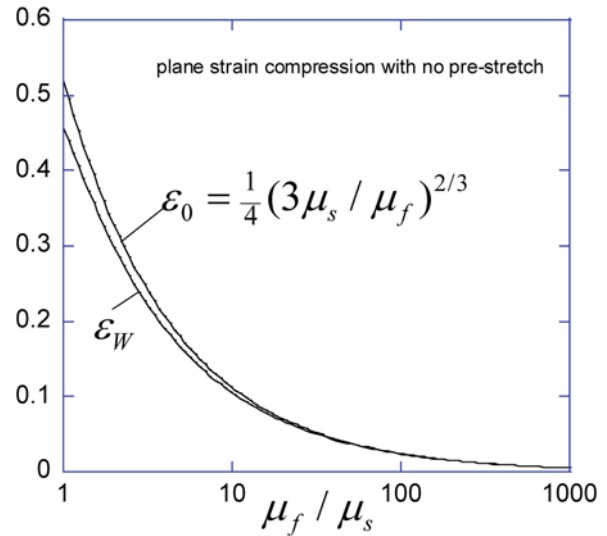


**Fig. 2 Compressive strain in the film at wrinkling,  $\varepsilon_W$ , as a function of the film/substrate modulus ratio of the two neo-Hookean materials for plane strain compression with no substrate prestretch. The prediction,  $\varepsilon_0$ , of the simple formula, Eq. (5), for wrinkling of a stiff linear elastic film on a compliant linear substrate is also shown.**

with bifurcation strains that are not small. For this to be true, the strain in Eq. (5) must be interpreted as the nominal strain defined in Eq. (4).

The limit for the homogeneous case ( $\mu_f/\mu_s = 1$ ) in Fig. 2 is  $\varepsilon_W = 0.456$  corresponding to Biot's [3] result for surface wrinkling of a homogeneous neo-Hookean half space under plane strain compression. Because there is no length scale associated with the homogeneous half-space, the surface bifurcation mode in this limit can have any wavelength.<sup>2</sup> As recent work [5] has shown, surface wrinkling of a homogeneous half-space is highly unstable and imperfection-sensitive such that compressive strains as large as  $\varepsilon_W = 0.456$  in the film are not likely to be achieved. Instead, finite strain creases in the film become energetically favorable when the compressive strain exceeds  $\varepsilon = 0.35$  in plane strain compression [6,7]. Thus, one can anticipate that the bifurcation result in Fig. 2 for  $\mu_f/\mu_s < 2$  is an upper bound in the sense that imperfections will trigger surface creases within the film before the wrinkling bifurcation mode can be attained. For larger

<sup>2</sup>In passing it is worth mentioning that surface wrinkling strain,  $\varepsilon_W = 0.456$ , is also the critical strain for wrinkling localized at the bonded interface between two semi-infinite half-spaces of neo-Hookean materials with different ground state moduli. This result, due to Biot, can be readily appreciated by noting that each half-space undergoes traction-free surface wrinkling at the same strain with arbitrary sinusoidal wavelength. Thus, the two wrinkled half-spaces can be "fit together" satisfying continuity of displacements and tractions.

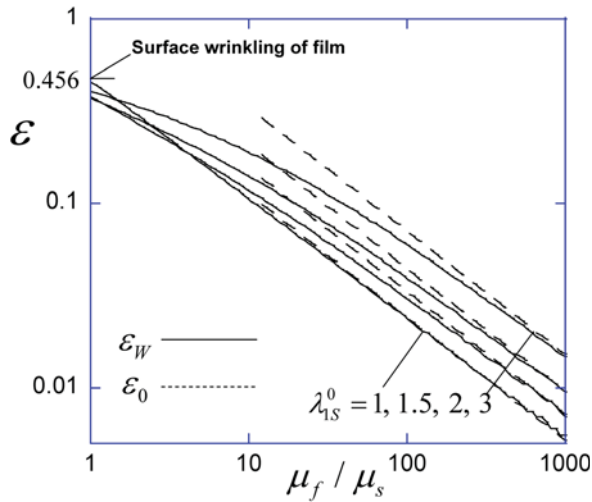


**Fig. 3** Compressive strain in the film at wrinkling,  $\varepsilon$ , as a function of the film/substrate modulus ratio of the two neo-Hookean materials for plane strain compression showing the influence of plane strain substrate prestretch,  $\lambda_{1s}^0$ . The prediction,  $\varepsilon_0$ , of the simple formula, Eq. (5), for wrinkling of a stiff linear elastic film on a compliant prestretched substrate is also shown. The range  $1 \leq \mu_f / \mu_s \leq 5$  is magnified in Fig. 4.

$\mu_f / \mu_s$  with smaller  $\varepsilon_W$ , the bifurcation mode has a unique wavelength proportional to the film thickness,  $h$ , as will be illustrated.

**3.2 Plane Strain Compression With Plane Strain Substrate Prestretch.** An undeformed film is attached to a substrate which has been subject to a prestretch,  $\lambda_{1s}^0 > 1$ , in plane strain with  $\lambda_{3s}^0 = 1$  and  $\lambda_{2s}^0 = 1/\lambda_{1s}^0$ . The film/substrate system subsequently undergoes incremental plane strain compression with decreasing  $\lambda_{1s}$  subject to  $\lambda_{3s} = 1$  and  $\lambda_{2s} = 1/\lambda_{1s}$ . The stretches in the film are given by Eq. (1). The effect of the prestretch on the critical compressive strain in the film,  $\varepsilon_W = 1 - \lambda_{1f}$ , at the onset of wrinkling is shown in Fig. 3. Included in this figure is the prediction of the simple formula, Eq. (5), which becomes increasing accurate for  $\mu_f / \mu_s \geq 10$ . Prestretch has a large effect on the wrinkling strain when the film is stiff compared to the substrate such that, for increasing prestretch,  $\varepsilon_W$  scales with  $\lambda_{1s}^{0\ 4/3}$ .

Prestretch produces anisotropic stiffening of the substrate (see Appendix) which increases the wrinkling strain when the film is stiff compared to the substrate as seen in Fig. 3. In the range in which the ground state modulus of the film is only slightly larger than that of the substrate, the prestretch has the unexpected effect of lowering the critical bifurcation strain. This is seen in Fig. 4 where the critical bifurcation strain  $\varepsilon_W$  is plotted for the same levels of prestretch for a much smaller range of  $\mu_f / \mu_s$ . With  $\mu_f / \mu_s = 1$  and no prestretch (i.e., an initially homogeneous substrate),  $\varepsilon_W = 0.456$ , corresponding to Biot's arbitrarily short wavelength surface mode as already noted. However, for all other combinations plotted in Fig. 4, the critical strain is below the Biot limit and the wavelength of the mode associated with the critical compressive strain has a wavelength that is long compared to the film thickness. Figure 5 further highlights this unusual influence of substrate prestretch for the case in which the ground state modulus of the film and the substrate are the same ( $\mu_f / \mu_s = 1$ ). In the range of prestretch,  $1 < \lambda_{1s}^0 < 5$ , the critical compressive strain in the film is less than the Biot strain and the wavelength of the critical mode is long compared to the film thickness. For prestretches greater than five, the Biot mode again becomes critical. This behavior appears anomalous given the stiffening that occurs in the substrate under prestretch. However, as the substrate becomes anisotropic, some of the incremental moduli components diminish. In addition, as the film is compressed it is incremental in-plane stiffness increases. Evidently, the very different anisotropies

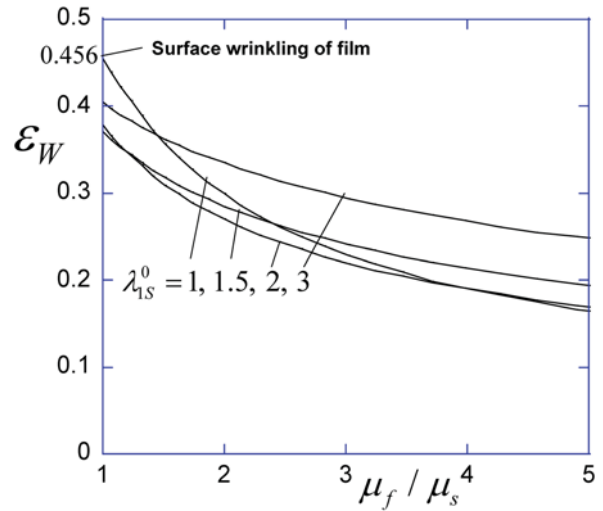


**Fig. 4** Compressive strain in the film at wrinkling,  $\varepsilon_W$ , as a function of the film/substrate modulus ratio of the two neo-Hookean materials for plane strain compression showing the influence of plane strain substrate prestretch,  $\lambda_{1s}^0$ , in the range in which the ratio of the film to substrate modulus is not large

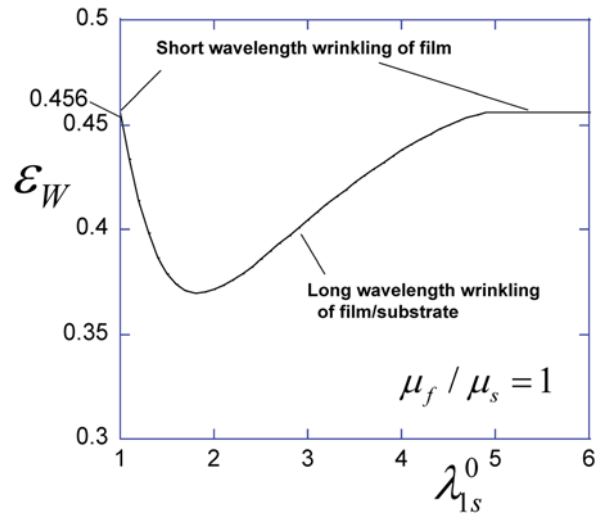


**Fig. 5** Compressive strain in the film at wrinkling,  $\varepsilon_W$ , for plane strain compression showing the influence of plane strain substrate prestretch,  $\lambda_{1s}^0$ , for neo-Hookean films and substrates that have the same ground state modulus ( $\mu_f / \mu_s = 1$ ). In the range of prestretch,  $1 < \lambda_{1s}^0 < 5$ , the critical mode is not the short wavelength surface mode but rather a mode with wavelength that is long compared to film thickness.

that develop in the film and the substrate account for the behavior in Fig. 5, but a simple explanation of the anomaly is not apparent.

The dimensionless wave number,  $kh$ , of the mode from the exact analysis for the cases shown in Fig. 3 is plotted in Fig. 6. The normal deflection of the mode is proportional to  $\cos(kx_1)$  where  $x_1$  is defined in Sec. 1. The wavelength of the mode in the deformed state is  $\ell = 2\pi\lambda_{1f}/k$ . The plot for  $\mu_f / \mu_s \geq 10$  includes the dimensionless wave number,  $k_0h$ , from Eq. (5) which becomes increasing accurate for large  $\mu_f / \mu_s$ . Prestretch also has an appreciable effect on the critical wave number such that it increases in proportion to  $\lambda_{1s}^{0\ 2/3}$  when the prestretch is relatively large.

**3.3 Uniaxial Compression With Uniaxial Stressing Prestretch.** To illustrate the role of the deformation history on wrinkling, consider uniaxial prestretching followed by uniaxial

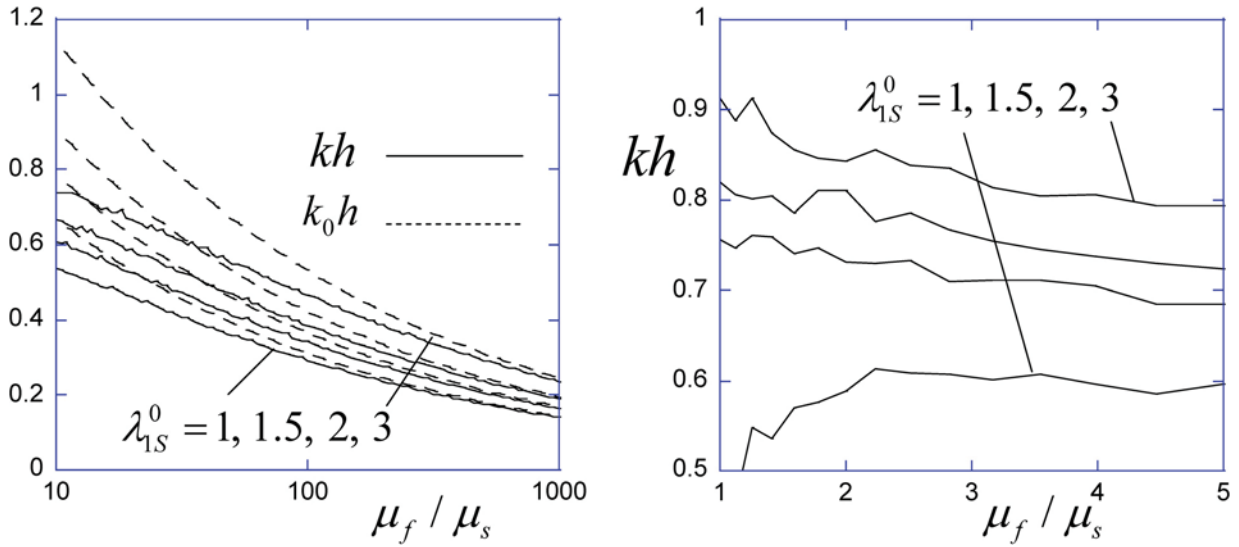


Fig. 6 Dimensionless wave number of the wrinkling mode as a function of the film/substrate modulus ratio of the two neo-Hookean materials for plane strain compression including the influence of plane strain substrate prestretch. The prediction,  $k_0h$ , from the simple formula, Eq. (5), for wrinkling of a stiff linear elastic film on a compliant prestretched substrate is also shown in the range of large stiffness ratio. The normal deflection of the top surface of the film has the form  $u_2 \propto \cos(kx_1)$  where  $x_1$  identifies material point locations in the undeformed film. Other than the limit for  $\mu_f/\mu_s = 1$  with  $\lambda_{1s}^0 = 1$  which is not plotted, the critical mode has a wavelength that is large compared to the film thickness.

compression, as is sometimes employed in wrinkling experiments. Specifically, consider prestretching of the substrate carried out under uniaxial tension such that  $\lambda_{1s}^0 > 1$  with  $\lambda_{2s}^0 = \lambda_{3s}^0 = 1/\sqrt{\lambda_{1s}^0}$ . Then, the film is attached to the substrate and the substrate is assumed to undergo incremental uniaxial compressive stressing under decreasing  $\lambda_{1s}$  with  $\lambda_{2s} = \lambda_{3s} = 1/\sqrt{\lambda_{1s}}$ . Film stretches are given by Eq. (1). The compressive wrinkling strain in the film,  $\varepsilon_w = 1 - \lambda_{1f}$ , at bifurcation is plotted in Fig. 7. The corresponding predictions from Eq. (2) for this case are

$$\varepsilon_0 = \frac{1}{3} \left( \Lambda \frac{3\mu_s}{\mu_f} \right)^{2/3}, \quad k_0h = \left( \Lambda \frac{3\mu_s}{\mu_f} \right)^{1/3} \quad \text{with} \quad (6)$$

$$\Lambda = \frac{1}{2} \lambda_{1s}^0{}^{1/2} \left( 1 + \lambda_{1s}^0{}^{3/2} \right)$$

(now with  $\nu_f = 1/2$ ,  $\bar{\mu}_f = \mu_f$ ,  $\varepsilon_0 = (4/3) \sigma/\bar{E}_f = \sigma/E_f$ ), and  $\varepsilon_0$  is included in Fig. 7.

The trends are similar to those for plane strain deformations. For moderately large prestretch  $\varepsilon_w$  again scales with  $\lambda_{1s}^0{}^{4/3}$ .

The wrinkling strain of the homogeneous substrate is  $\varepsilon_w = 0.556$  under uniaxial stressing conditions with no prestretch. Biot's [3] result for surface wrinkling bifurcation of a homogeneous neo-Hookean substrate under general uniform stretching is

$$\varepsilon_w = 1 - 0.5437/\sqrt{\lambda_3} \quad (7)$$

for conditions in which the maximum compressive stress acts in the 1-direction. This result provides the values quoted above for plane strain and uniaxial stressing. Under uniaxial stressing, substrate prestretch causes only a slight reduction of the critical strain in the domain of modulus ratios near unity (Fig. 7).

#### 4 Numerical Analysis of Post-Bifurcation Modes Under Plane Strain

A finite element model has been employed to investigate plane strain compression of the neo-Hookean bilayer at compressive strain levels well beyond the bifurcation strain. Advanced post-bifurcation modes are revealed for cases with and without

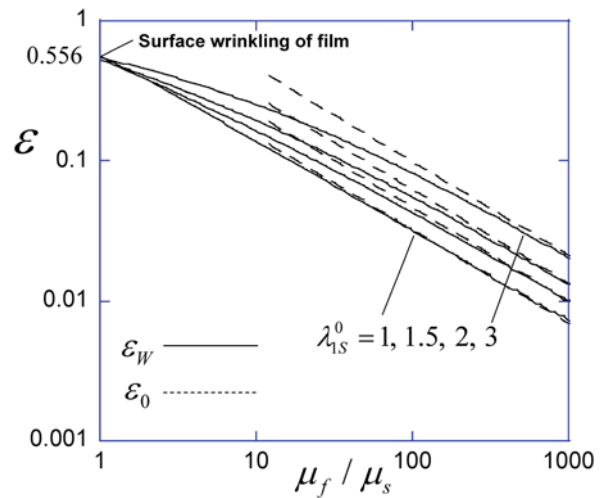


Fig. 7 Compressive strain in the film at wrinkling,  $\varepsilon_w$ , as a function of the film/substrate modulus ratio of the two neo-Hookean materials for uniaxial compression showing the influence of substrate prestretch under uniaxial tension. The prediction,  $\varepsilon_0$ , of the simple formula, Eq. (6), for wrinkling of a stiff linear elastic film on a compliant prestretched substrate is also shown.

substrate prestretch. Plane strain ( $\lambda_{2f} = \lambda_{3s} = 1$ ) finite element simulations have been performed via the commercial software, ABAQUS [8]. The ratio of the anticipated wavelength to the element size is taken to be approximately 100. In the finite element simulations, the incompressible neo-Hookean material model is employed for both the film and the substrate. The hybrid element (CPE6MH in ABAQUS) suitable for simulations of incompressible materials is adopted. Two schemes are adopted to introduce initial stress-free geometric surface imperfections. For the case of no substrate prestretch, a linear perturbation procedure is accomplished using the "buckle" function in the software. The critical eigenmode scaled by a very small factor ( $\approx 0.005h$ ) is introduced as a geometric imperfection into the mesh. For the case in which the substrate is prestretched, finite element simulations are first



run by specifying a displacement  $u_2 = 0.025h \cos(kx_1)$  at the upper surface, where  $k$  is the anticipated wave number. The computed displacement field is introduced as a stress-free geometric imperfection into the mesh.

In the post-buckling analysis, displacement-controlled loading is employed with  $u_1$  (independent of  $x_2$ ) and zero shear traction specified on the vertical sides of the model. The nominal compressive overall strain applied to the system after the film is attached to the substrate,  $\varepsilon$ , is defined exactly as in Eq. (4) in terms of the film stretch,  $\lambda_{1f}$ , evaluated in terms of the difference between  $u_1$  on the two sides of the model. On the bottom surface,  $u_2$  and the shear traction are taken to be zero. The width of the model is taken to be on the order of 5–10 wavelengths of the sinusoidal wrinkling mode, as will be evident from the deflection patterns. The depth of the substrate is taken to be more than ten times the sinusoidal wavelength and; thus, sufficiently deep to ensure that there is no interaction with the modes and the bottom of the substrate—effectively, the substrate is infinitely deep. The numerical model relies on the slight initial geometric imperfection to initiate growth of the post-bifurcation modes.

It is not straightforward to simulate plane strain compression with substrate prestretch with the finite element software because of the necessity of specifying the mesh in advance. If a regular mesh is imposed on the bilayer followed by substrate prestretch, the film elements can be rendered inactive using the function, “model change, remove,” but the resulting mesh in the film winds up highly distorted before the compression phase begins. This problem can be circumvented using features available in the software by the following steps. A background mesh is designed which shares nodes with the film mesh and which has a uniform ground state shear modulus. The entire film/substrate is then pre-stretched to the desired substrate prestretch. In this way, the mesh in the film deforms with the substrate. Before compression of both film and the substrate, the background mesh can be removed with the function, “model change, remove”. Using the function, “model change, add,” one can reactivate the film mesh, set the state of the film to be stress-free, and re-set the ground state modulus of the substrate to its correct value,  $\mu_s$ . From this point, the system is subject to increments of plane strain compression.

**4.1 Plane Strain Compression With No Substrate Prestretch.** Numerical simulations have been performed for the bilayer modulus ratio in the range  $3 \leq \mu_f/\mu_s \leq 80$  with results displayed in Fig. 8. The linear perturbation analysis using the “buckle” function in the software allows direct computation of  $\varepsilon_W$ , corresponding to the onset of the sinusoidal wrinkling mode. It is in good agreement with the result of Sec. 3.1.

Two very different post-bifurcation modes are observed depending on  $\mu_f/\mu_s$ . When  $\mu_f/\mu_s$  is large, the sinusoidal wrinkling mode is stable to strains that can be many times  $\varepsilon_W$  (see Fig. 9). Then, at a compressive strain denoted by  $\varepsilon_{PD}$  in Fig. 8, the sinusoidal mode transitions into a mode with twice the wavelength (see Fig. 9). This period-doubling mode would occur as a secondary bifurcation in a perfect system, but in the present simulations it is triggered by slight imperfections. The precise value of  $\varepsilon_{PD}$  is difficult to pin down in the simulations, as evident from the small variations in Fig. 8. For this bilayer system it is noted that  $\varepsilon_{PD} \cong 0.2$  for all  $\mu_f/\mu_s \geq 10$ . For stiff films, the sinusoidal wrinkling mode is highly stable for relatively large compressions prior to the onset of period-doubling, as illustrated in Fig. 9. A combined analytical-experimental study [9] of the nonlinear evolution of the sinusoidal wrinkling mode prior to period-doubling has been carried for stiff films on compliant neo-Hookean substrates. Studies of period-doubling for stiff thin films on compliant elastomer substrates, including experimental realizations of the mode, have been presented in Refs. [4] and [10]. In addition, period-doubling in wrinkling has been also been identified in the system of a cylindrical cavity covered by a stiff surface layer [11].

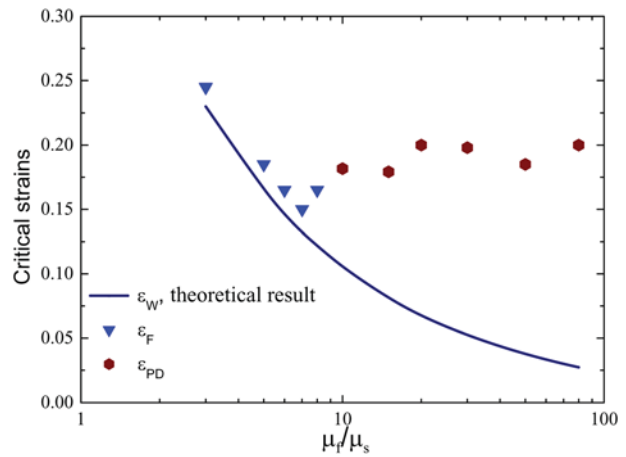


**Fig. 8 Post-bifurcation behavior in the neo-Hookean bilayer under plane strain compression with no substrate prestretch computed using the finite element model. The critical compressive strain at the onset of wrinkling,  $\varepsilon_W$ , is the theoretical result of Sec. 3.1. The compressive strain at the onset of two distinct post-bifurcation modes is also indicated. For  $\mu_f/\mu_s \geq 10$ , period-doubling (see Fig. 9) is the first post-bifurcation mode encountered at strain  $\varepsilon_{PD}$ . For  $\mu_f/\mu_s < 10$ , the post-bifurcation mode is a fold that occurs at a strain denoted by  $\varepsilon_F$  that is only slightly greater than  $\varepsilon_W$ . It subsequently develops a local crease (see Fig. 10).**

For  $\mu_f/\mu_s < 10$ , the post-bifurcation mode changes to what will be called a “folding mode” at a strain denoted by,  $\varepsilon_F$ , that is only slightly above  $\varepsilon_W$ , as seen in Fig. 8. The steps involved in the formation of the folding mode are illustrated by the example in Fig. 10. A localization develops within the multiple undulations of the sinusoidal mode where, in the example in Fig. 10, two neighboring undulations grow relative to all the others—a distinct two-lobed undulation develops. With a slight further increase of overall compression, the localization process continues as one of the two undulations becomes dominant in the form of an incipient fold. Then, at the deepest point on this incipient fold, a crease is

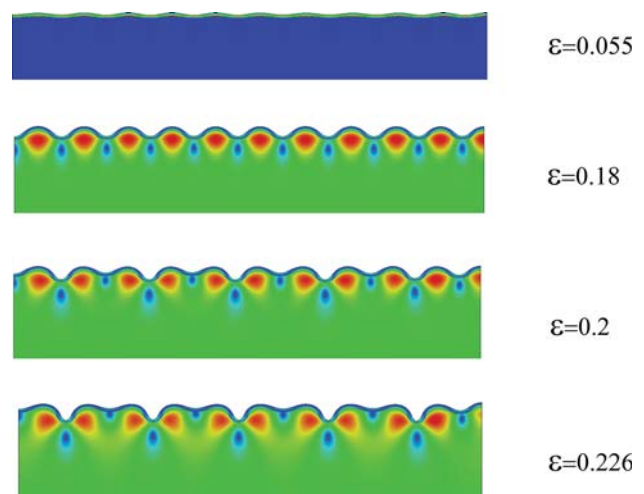


**Fig. 9 Plane strain compression with  $\mu_f/\mu_s = 30$  and no substrate prestretch. Bifurcation first occurs as a sinusoidal wrinkling mode ( $\varepsilon \cong 0.055$ ). The sinusoidal mode is stable to much larger strains (e.g.,  $\varepsilon = 0.18$ ). At a compressive strain of approximately  $\varepsilon = 0.2$  a secondary bifurcation occurs corresponding to the onset of period doubling. With a slight further increase of compression to  $\varepsilon = 0.226$  the period-doubling mode is firmly established. This behavior is representative of bilayers with  $\mu_f/\mu_s > 10$  if there is no prestretch.**

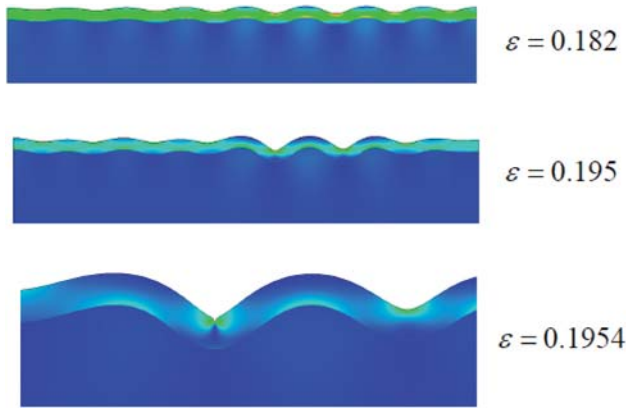


Fig. 10 Plane strain compression with  $\mu_f/\mu_s = 5$  and no substrate prestretch. Bifurcation into the sinusoidal wrinkling mode occurs at  $\varepsilon \cong 0.175$ . Already at a strain slightly above the onset of bifurcation ( $\varepsilon = 0.182$ ) the deflection is showing signs that it is evolving away from the sinusoidal mode. At  $\varepsilon = 0.195$  the film deflection has localized into two side-by-side incipient folds. With a slight additional increase in strain ( $\varepsilon = 0.1954$ ) the fold on the left becomes dominant and a crease has begun to form in the film at the point of maximum local compression. This behavior is representative of bilayers with  $\mu_f/\mu_s < 10$  and no prestretch.

nucleated at the film surface. The simulation is terminated at this point. The localized folding mode was observed in all the simulations performed in the range  $3 \leq \mu_f/\mu_s < 10$ .

**4.2 Plane Strain Compression With Modest Substrate Prestretch,  $\lambda_{1s}^0 = 1.3$ .** When the substrate prestretch is relatively small as in Fig. 11, the behavior is qualitatively similar to that just described for the case on no prestretch. The prestretch shifts the transition from folding to period-doubling to somewhat larger  $\mu_f/\mu_s$  and, more significantly, it delays the onset of the double-period mode to larger strains. An example of evolution of the sinusoidal mode to the period-doubling mode for  $\mu_f/\mu_s = 186$  is given in Fig. 12.

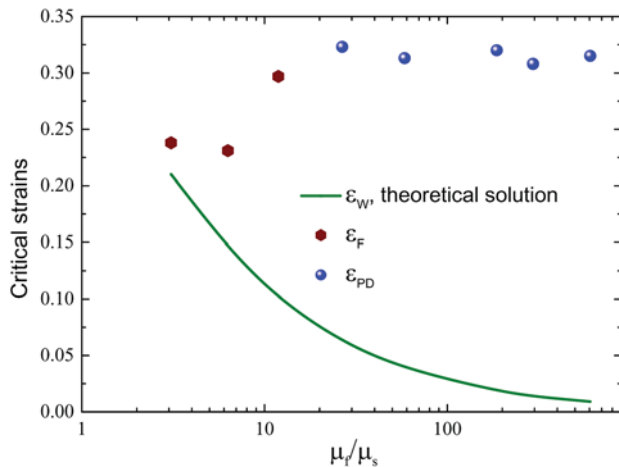


Fig. 11 Numerical simulations of the post-bifurcation modes for plane strain compression with a relatively small plane strain prestretch of the substrate,  $\lambda_{1s}^0 = 1.3$ . The curve for the bifurcation strain,  $\varepsilon_W$ , at the onset of sinusoidal wrinkling is that from the theoretical calculation in Sec. 3.2. The post-bifurcation behavior with small prestretch is qualitatively similar to the case with no prestretch, although the secondary modes are delayed to larger overall compressive strains. Period-doubling occurs when  $\mu_f/\mu_s \geq 20$  (see Fig. 12) with folding at smaller values of the modulus ratio.

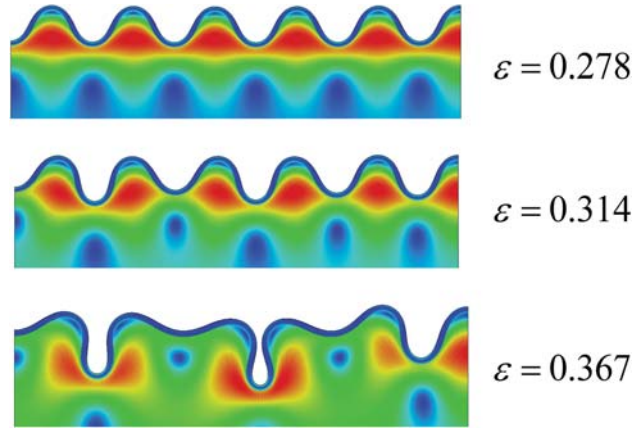


Fig. 12 Evolution of wrinkling mode under plane strain compression with a plane strain substrate prestretch  $\lambda_{1s}^0 = 1.3$  for  $\mu_f/\mu_s = 186$ . The sinusoidal wrinkling mode associated with bifurcation at  $\varepsilon_W = 0.019$  is stable to much larger strains (e.g.,  $\varepsilon = 0.278$  above). The onset of period-doubling is evident at  $\varepsilon = 0.314$  and is fully developed at  $\varepsilon = 0.367$ .

**4.3 Plane Strain Compression With “Large” Substrate Prestretch,  $\lambda_{1s}^0 = 2$ .** The behavior described above changes dramatically for a larger prestretch,  $\lambda_{1s}^0 = 2$ . In this case, an entirely different mode is observed at compressive strains in the film that are only modestly larger than the bifurcation strain,  $\varepsilon_W$ , as seen in Figs. 13 and 14. For the entire range of modulus ratio for which the simulations have been performed,  $4 \leq \mu_f/\mu_s \leq 1000$ , the secondary mode observed is the “mountain ridge mode,” labeled so for reasons that will be evident from the mode shape in Fig. 14. Like the folding mode, this mode is a compressive localization. As the ridge forms, it relaxes the compression in the film on both sides of itself and thereby reduces the amplitudes of the wrinkles in its neighborhood. Similar stress relaxation is seen for on either side of a buckle delamination when the film

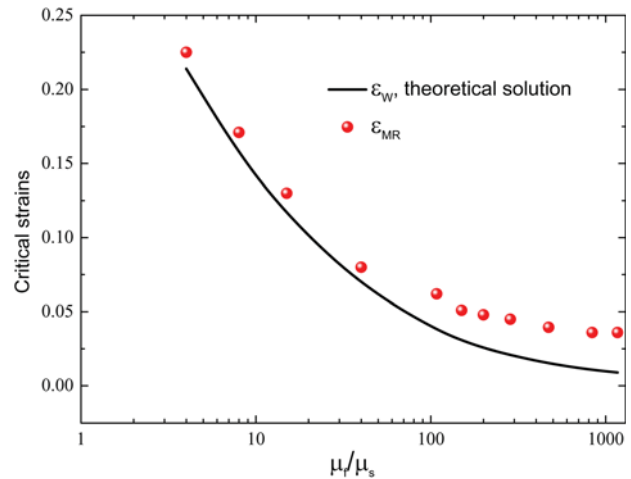
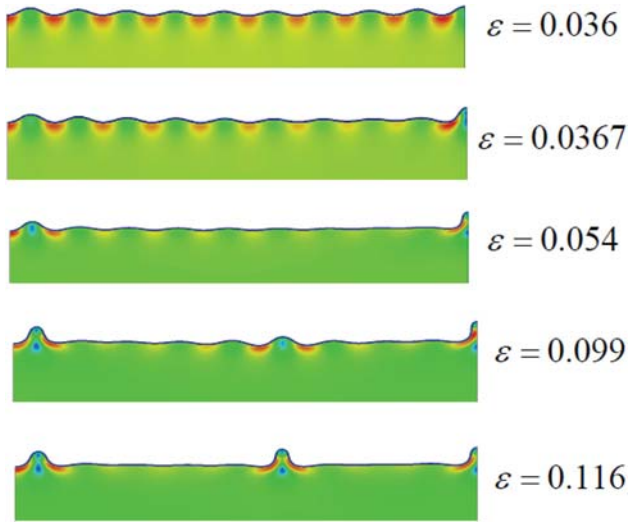


Fig. 13 Numerical simulations of the post-bifurcation modes for plane strain compression with a plane strain prestretch of the substrate,  $\lambda_{1s}^0 = 2$ . The curve for the bifurcation strain,  $\varepsilon_W$ , at the onset of sinusoidal wrinkling is that from the theoretical calculation in Sec. 3.2. For this level of prestretch the secondary post-bifurcation mode is the mountain ridge mode (see Fig. 14) at all values of  $\mu_f/\mu_s$  plotted. The compressive strain at its onset is denoted by  $\varepsilon_{MR}$ . In the range where  $\mu_f/\mu_s$  is not large, mountain ridges form with relatively small additional compression after bifurcation. When  $\mu_f/\mu_s$  is large, mountain ridges form at compressive strains that are small and roughly twice  $\varepsilon_W$ .



**Fig. 14 Evolution of wrinkling mode under plane strain compression with a plane strain substrate prestretch  $\lambda_{1s}^0 = 2$  for  $\mu_f/\mu_s = 836$ . The sinusoidal wrinkling mode associated with bifurcation at  $\varepsilon_W \cong 0.01$  is stable to  $\varepsilon = 0.036$  but at  $\varepsilon = 0.0367$  a mountain ridge has formed at the right end of the model and the amplitude of the undulations near the ridge have been reduced. By  $\varepsilon = 0.054$  a second mountain ridge is clearly forming near the left end, and by  $\varepsilon = 0.099$  this ridge is fully developed with a third ridge beginning to emerge near the center. At  $\varepsilon = 0.116$  three fully developed mountain ridges have formed and have relaxed the undulation amplitudes between the ridges. The ridges are a form of localization under compression.**

is sufficiently stiff compared to the substrate [12]. As seen in Fig. 14, further overall compression causes more mountain ridges to form. For stiff films ( $\mu_f/\mu_s = 836$  in Fig. 14), the overall compressive strains at which the mountain ridges form are not nearly as large as the strains required for period-doubling seen in Figs. 8 and 11 for the other cases. Thus, this phenomenon should be expected for any linear elastic film material.

## 5 Conclusions

The neo-Hookean film/substrate bilayer admits a rich variety of wrinkling modes, especially when prestretch of the substrate is considered. In all cases, the first mode to appear as the bilayer is compressed is the sinusoidal wrinkling mode associated with bifurcation from the bi-uniform state. The compressive strain in the film at bifurcation,  $\varepsilon_W$ , depends on the substrate prestretch,  $\lambda_{1s}^0$ , as well as the ground state modulus ratio,  $\mu_f/\mu_s$ . For systems with a modest stiffness difference between the film and substrate (e.g.,  $1 < \mu_f/\mu_s < 10$ ), the bifurcation strain is relatively large and no doubt strongly dependent on the fact that the film has been taken to be a neo-Hookean material. For stiffer films, the bifurcation strain is relatively small such that it and its associated mode should be applicable to any linear elastic film material. When the film is stiff (i.e.,  $\mu_f/\mu_s \geq 100$ ), the simple formula, Eq. (2), generalizes the well known formula of Allen [1] to account for the fact that the incremental moduli of the prestretched substrate are different from its ground state moduli. This formula applies specifically to neo-Hookean substrates but is expected to reflect the role of prestretch for any elastomeric material that stiffens as it is stretched.

The second mode to appear as the system is compressed beyond bifurcation can be one of several advanced post-bifurcation modes, including folding, period-doubling and mountain ridging. Folding and mountain ridging involve a localization process in which the local deflection of the film relaxes compression in its

neighborhood thereby growing at the expense of the undulations in its neighborhood. Which one of the advanced mode to appear depends on the combination of the ground state modulus ratio,  $\mu_f/\mu_s$ , and substrate prestretch,  $\lambda_{1s}^0$ . The set of numerical simulations presented here have been limited to two levels of prestretch, although a selected number of additional simulations at other prestretches indicate that the modes reported in Sec. 4 are not isolated events. It remains for further work to perform a more exhaustive set of simulations that would map the occurrence of the advanced modes as a function of ground state modulus ratio, substrate prestretch and overall compression. Prestretch induces anisotropic incremental moduli in the substrate, increasing some components and decreasing others. The anisotropic moduli play an important role in selecting the advanced mode, and these moduli depend on the constitutive model of the substrate. Thus, to an extent which is not yet established, the occurrence of the various advanced modes revealed here may differ for other substrate constitutive models.

To our knowledge, there have been no reported experimental observations of the mountain ridge mode in the literature related to stiff films on compliant elastomer substrates, but it is possible that experiments have not yet been performed in the relevant range of prestretch. The mountain ridge mode occurs at relative small compressive strains for stiff films. Thus, it should be realizable for any linear elastic film material on a substrate can be reasonably approximated as a neo-Hookean material.

## Acknowledgment

Y.P.C. acknowledges the financial support from Tsinghua University (Grant No. 2009THZ02122).

## Appendix

**Bifurcation Analysis of Neo-Hookean Bilayer.** The equations governing the bifurcation problem are constructed from exact solutions for increments of displacements and stresses in a uniformly stretched layer. Let  $\lambda_i$ ,  $i = 1, 3$  be the uniform stretches with  $\lambda_1 \lambda_2 \lambda_3 = 1$  and  $r = \lambda_2/\lambda_1$ . In a finite thickness, neo-Hookean layer with ground state shear modulus  $\mu$ , separated solutions to the field equations for the incremental problem exist with displacement increments,  $(u_1, u_2) = (U_1 \sin(kx_1), U_2 \cos(kx_1))$ , given by

$$\begin{aligned} U_1 &= -c_1 e^{rkx_2} - c_2 r^{-1} e^{kx_2} + c_3 e^{-rkx_2} + c_4 r^{-1} e^{-kx_2} \\ U_2 &= c_1 e^{rkx_2} + c_2 e^{kx_2} + c_3 e^{-rkx_2} + c_4 e^{-kx_2} \end{aligned} \quad (A1)$$

assuming  $r \neq 1$ . This representation is degenerate for  $r = 1$ , but the solution for this limit is not required here. Note that the current stretch state enters, Eq. (A1), only through  $r$ . The solution holds for any  $k$ . The Cartesian coordinates  $(x_1, x_2)$  label material points in the undeformed layer and the displacement increments are with respect to this coordinate system. Nominal stress increments,  $(n_{21}, n_{22}) = (N_{21} \sin(kx_1), N_{22} \cos(kx_1))$ , with components referred to the same coordinate system and defined as force per undeformed area, are given by

$$\begin{aligned} N_{21} &= -\mu k [c_1 2r e^{rkx_2} + c_2 r^{-1} (r^2 + 1) e^{kx_2} + c_3 2r e^{-rkx_2} \\ &\quad + c_4 r^{-1} (r^2 + 1) e^{-kx_2}] \\ N_{22} &= -\mu k [-c_1 r^{-1} (r^2 + 1) e^{rkx_2} - c_2 2e^{kx_2} + c_3 r^{-1} (r^2 + 1) e^{-rkx_2} \\ &\quad + c_4 2e^{-kx_2}] \end{aligned} \quad (A2)$$

This Lagrangian formulation, which employs the components of the second Piola-Kirchhoff stress, is the same used in the study of the stability of wrinkling of a homogeneous half-space [5]. The



reader is referred to Ref. [5] or to Biot's book [13] for background details.

For the film layer, with  $0 \leq x_2 \leq h$ ,  $\mu = \mu_f$  and  $r = r_f = \lambda_{2f}/\lambda_{1f}$ , enforce  $(N_{21}, N_{22}) = 0$  on  $x_2 = h$  to obtain  $(c_3, c_4)$  in terms of  $(c_1, c_2)$ :

$$\begin{bmatrix} c_3 \\ c_4 \end{bmatrix} = A \begin{bmatrix} c_1 \\ c_2 \end{bmatrix} \quad (\text{A3})$$

$$\text{with } A = \begin{bmatrix} 2re^{-rkh} & r^{-1}(r^2+1)e^{-kh} \\ r^{-1}(r^2+1)e^{-rkh} & 2e^{-kh} \end{bmatrix}^{-1} \\ \times \begin{bmatrix} -2re^{rkh} & -r^{-1}(r^2+1)e^{kh} \\ r^{-1}(r^2+1)e^{rkh} & 2e^{kh} \end{bmatrix}$$

Then solve for  $(N_{21}, N_{22})$  on  $x_2 = 0^+$  in terms of  $(c_1, c_2)$ :

$$\begin{bmatrix} N_{21} \\ N_{22} \end{bmatrix} = \mu_f k B \begin{bmatrix} c_1 \\ c_2 \end{bmatrix} \quad (\text{A4})$$

with  $B$

$$= \begin{bmatrix} -2r(1+A_{11}) - r^{-1}(r^2+1)A_{21} & -r^{-1}(r^2+1)(1+A_{22}) - 2rA_{12} \\ r^{-1}(r^2+1)(1-A_{11}) - 2A_{21} & 2(1-A_{22}) - r^{-1}(r^2+1)A_{12} \end{bmatrix}$$

Next, solve for  $(U_1, U_2)$  on  $x_2 = 0^+$  in terms of  $(c_1, c_2)$  using (A1) and (A3):

$$\begin{bmatrix} U_1 \\ U_2 \end{bmatrix} = C \begin{bmatrix} c_1 \\ c_2 \end{bmatrix} \text{ with} \\ C = \begin{bmatrix} -1 + A_{11} + r^{-1}A_{21} & -r^{-1} + A_{12} + r^{-1}A_{22} \\ 1 + A_{11} + A_{21} & 1 + A_{12} + A_{22} \end{bmatrix} \quad (\text{A5})$$

By Eqs. (A4) and (A5), the increments of nominal stress and displacement on the bottom of the film layer having a traction-free top surface are related by

$$\begin{bmatrix} N_{21} \\ N_{22} \end{bmatrix} = \mu_f k B C^{-1} \begin{bmatrix} U_1 \\ U_2 \end{bmatrix} \quad \text{on } x_2 = 0^+ \quad (\text{A6})$$

Now consider the semi-infinite substrate. If the substrate has a prestretch,  $\lambda_{1s}^0$ , relative to the film, the coordinate in the substrate relative to its undeformed state is  $\bar{x}_1 = x_1/\lambda_{1s}^0$ . Continuity of increments of traction and displacement across the interface require

$$\frac{1}{\lambda_{1s}\lambda_{3s}}(N_{21} \sin(\bar{k}\bar{x}_1), N_{22} \cos(\bar{k}\bar{x}_1))^- \\ = \frac{1}{\lambda_{1f}\lambda_{3f}}(N_{21} \sin(kx_1), N_{22} \cos(kx_1))^+ \quad (\text{A7})$$

$$(U_1 \sin(\bar{k}\bar{x}_1), U_2 \cos(\bar{k}\bar{x}_1))^- = (U_1 \sin(kx_1), U_2 \cos(kx_1))^+ \quad (\text{A8})$$

One condition is  $\bar{k}\bar{x}_1 = kx_1$  and; thus,  $\bar{k} = \lambda_{1s}^0 k$ . The factors,  $1/\lambda_{1s}\lambda_{3s}$ , multiplying the increments in Eq. (A7) account for the fact that the nominal stress increments in the two layers are defined relative to different undeformed areas if the substrate has a prestretch.

The separated solution, Eq. (A1), applies to the semi-infinite substrate with  $\mu = \mu_s r = r_s = \lambda_{2s}/\lambda_{1s}$ ,  $k \rightarrow \bar{k}$  and  $c_3 = c_4 = 0$ . It is straightforward to show that the relation between  $(N_{21}, N_{22})$  and  $(U_1, U_2)$  on the top of the substrate ( $x_2 = 0^-$ ) is

$$\begin{bmatrix} N_{21} \\ N_{22} \end{bmatrix} = \mu_s \bar{k} D \begin{bmatrix} U_1 \\ U_2 \end{bmatrix} \quad \text{with } D = \begin{bmatrix} r_s + 1 & -(r_s - 1) \\ -(r_s - 1) & r_s^{-1}(r_s + 1) \end{bmatrix} \quad (\text{A9})$$

The last step is to enforce continuity of traction and displacement increments across the interface, Eqs. (A7) and (A8), using (A6), (A9) and (1); this requires

$$(U_1, U_2)^+ = (U_1, U_2)^- \equiv (U_1, U_2)$$

and

$$E \begin{bmatrix} U_1 \\ U_2 \end{bmatrix} = 0 \quad \text{with } E = B C^{-1} - \frac{1}{\lambda_{3s}^0} \frac{\mu_s}{\mu_f} D \quad (\text{A10})$$

The eigenvalue problem governing bifurcation is  $|E| = 0$ . The eigenvalue associated with the critical compressive strain must be minimized over all values of  $kh$ . The solution to the eigenvalue problem is carried out numerically.

### Effect of Substrate Prestretch on Wrinkling Bifurcation of Stiff Films.

The extension, Eq. (2), of Allen's result [1] employs the relation, Eq. (A9) between the increments of traction and displacement as the elastic foundation onto which a compressed thin stiff plate is attached. With incremental normal and tangential displacements to the plate/substrate interface given by  $(u_1, u_2) = (U_1 \sin(k_0 x), U_2 \cos(k_0 x))$ , the resisting traction increments of the foundation are  $(t_1, t_2) = (T_1 \sin(k_0 x), T_2 \cos(k_0 x))$  where, by (A9),

$$\begin{bmatrix} T_1 \\ T_2 \end{bmatrix} = \frac{\mu_s k_0}{\lambda_{3s}^0} D \begin{bmatrix} U_1 \\ U_2 \end{bmatrix} \quad (\text{A11})$$

Here, the traction increments have been transformed to force per unit area of the plate in the current compressed state;  $D$  is given in Eq. (A9) with  $r_s = \lambda_{2s}^0/\lambda_{1s}^0$ . The separated equations governing the incremental deformation of the compressed plate are

$$\bar{E}_f h k_0^2 U_1 = -T_1 \\ ((\bar{E}_f h^3/12)k_0^4 - \sigma h k_0^2) U_2 = -T_2 + \alpha T_1 k_0 h/2 \quad (\text{A12})$$

where  $\bar{E}_f = E_f/(1 - \nu_f^2)$ ,  $\sigma$  is the compressive stress in the plate,  $h$  is its thickness, and  $\alpha = 1$  with the interface at the bottom of the plate and  $\alpha = 0$  if one imagines (as an approximation) that the mid-surface of the plate is attached to the top of the substrate. Here, we will be content in using the same approximations implicit in Allen's analysis by ignoring the coupling between the two equations in Eq. (A12), i.e., by focusing on the second equation with  $\alpha = 0$  and neglecting the contribution of  $U_1$ . The result after minimizing  $\sigma$  with respect to  $k_0$  is Eq. (2). The fully coupled equations, Eq. (A12), with  $\alpha = 1$  can be used to generate more accurate predictions than the extension in Eq. (2), as illustrated in Ref. [14] for the case of no substrate prestretch.

### References

- [1] Allen, H. G., 1969, *Analysis and Design of Sandwich Panels*, Pergamon, New York.
- [2] Crosby, A. J. (ed.), 2010, "Theme Issue: The Physics of Buckling," *Soft Matter* **6**, pp. 5647–5878.
- [3] Biot, M. A., 1963, "Surface Instability of Rubber in Compression," *Appl. Sci. Res.*, **12**, pp. 168–182.
- [4] Sun, J. Y., Xia, S., Moon, M.-Y., Oh, K. H., and Kim, K. S., 2011, "Folding Wrinkles of a Thin Stiff Layer on a Soft Substrate," *Proc. R. Soc. London, Ser. A*, **468**, pp. 932–953.
- [5] Cao, Y., and Hutchinson, J. W., 2012, "From Wrinkles to Creases in Elastomers: The Instability and Imperfection-Sensitivity of Wrinkling," *Proc. R. Soc. London, Ser. A*, **468**, pp. 94–115.
- [6] Holfeld, E. B., and Mahadevan, L., 2011, "Unfolding the Sulcus," *Phys. Rev. Lett.*, **106**, pp. 105702-1–105702-4.



- [7] Hong, W., Zhao, X., and Suo, Z., 2009, "Formation of Creases on the Surfaces of Elastomers and Gels," *App. Phys. Lett.*, **95**, pp. 111901-1-111901-3.
- [8] *ABAQUS Analysis User's Manual*, Version 6.8 (Simula, 2008).
- [9] Song, J., Jiang, H., Liu, Z. J., Khang, D. Y., Huang, Y., Rogers, J. A., Lu, C., and Koh, C. G., 2008, "Buckling of a Stiff Thin Film on a Compliant Substrate in Large Deformation," *Int. J. Solids Struct.*, **45**, pp. 3107-3121.
- [10] Brau, F., Vandeparre, H., Sabbah, A., Poulard, C., Boudaoud, A., and Damman, P., 2010, "Multiple-Length-Scale Elastic Instability Mimics Parametric Resonance of Nonlinear Oscillators," *Nature Mater.*, **7**, pp. 56-60.
- [11] Li, B., Cao, Y. P., Feng, X. Q., and Gao, H. J., 2011, "Surface Wrinkling of Mucosa Induced by Volumetric Growth: Theory, Simulation and Experiment," *J. Mech. Phys. Solids*, **59**, pp. 758-774.
- [12] Mei, H., Landes, C. M., and Huang, R., 2011, "Concomitant Wrinkling and Buckle-Delamination of Elastic Thin Films on Compliant Substrates," *J. Mech. Mater. Struct.*, **43**, pp. 627-642.
- [13] Biot, M. A., 1965, *Mechanics of Incremental Deformation*, Wiley, New York.
- [14] Cai, S., Breid, D., Crosby, A. I., Suo, Z., and Hutchinson, J. W., 2011, "Periodic Patterns and Energy States of Buckled Films on Compliant Substrates," *J. Mech. Phys. Solids*, **59**, pp. 1094-1114.